TURF-BOX: an active lighting multispectral imaging system with led VIS-NIR sources for monitoring of vegetated surfaces

A. Motisi[a], G. Impollonia, M. Minacapilli, S. Orlando and M. Sarno

University of Palermo, Department of Agricultural, Food and Forest Sciences, Viale delle Scienze, Bldg. 4, 90128 Palermo, Italy.

Abstract

A microcontroller driven system suitable to monitor soil and low vegetation is described. A radiometrically pre-calibrated imaging camera driven by a microcontroller is contained in a light-tight box aiming at an actively illuminated target surface area of 50×38 cm, using LED sources with different emission wavelengths (blue, green, red and infrared). The adopted arrangement allows measurements independent from local lighting conditions and from the in situ, per-session calibrations necessary with the conventional instrumentation adopted for field measurements. Sequential lighting of the target surface with the monochromatic LED sources allows capturing multispectral images at a relatively high resolution (1269×972 px) in the broadband visible (VIS, 420-670 nm), monochromatic (blue, green, red) and near-infrared (NIR, 820 nm) domains, useful for the characterization of surfaces of different nature such as soil, turf, and low-vegetation. A specialized firmware implements, in a web-based user interface, functions for estimation of standard spectral parameters and vegetation indices, suitable for the characterization of vegetated surfaces and the diagnosis of specific conditions, anomalies or pathologies. The system is intended for use both in a research environment and in the technical management of recreation or cultivated surfaces, both for direct use and as a calibrated reference in support to proximal-sensing and/or drone-based applications.

Keywords: multispectral camera, vegetation indices, NDVI, image analysis, spectral reflectance

INTRODUCTION

In agriculture, a common and widely used approach to analyze the spatial and temporal dynamics of biomass over large areas is based on the estimation of vegetation indices (VIs) from the spectral signature of a vegetated target. These indices can be obtained from remote or proximal sensing by multispectral systems, able to capture images in specific spectral bands, usually centered in VIS and NIR regions, as the widely used normalized difference vegetation index (NDVI) generally applied to map, at various observation scales, crop variables like leaf area index (LAI), plant coverage and chlorophyll (Aparicio et al., 2000). Similar approaches were also applied at different scale for fast and accurate estimates of a large number of soil properties such as particle size distribution, organic matter content, electrical conductivity, etc. (Viscarra Rossel et al., 2006; Maltese et al., 2010).

However, in order to fully exploit data provided from any sensor that operates in the solar spectral domain, the issue of the "reflectance calibration" must be addressed by supplemental ancillary information. The correct analysis of data acquired in VIS, NIR and/or IR spectral domains requires different pre-processing steps to remove bias and effects due to changes in atmospheric conditions during acquisition, changes in illumination during measurements (Berra et al., 2016) as well as to perform the conversion from the signal

[a]E-mail: antonio.motisi@unipa.it

measured by the sensor (radiance at sensor) to surface reflectance of the observed target.

In this paper, the design of a new multispectral system, called 'TURF-BOX', based on open-source software and low cost hardware is presented, which in part could be a possible solution for the aforementioned requirement. The system allows the capture of radiometrically corrected reflectance images in the VIS-NIR spectral domain (four bands centered in blue, green, red and near-infrared spectral regions), characterized by a resolution of 1296×972 pixels and designed to characterize spectral properties of soils and low vegetation. The TURF-BOX uses a suitable LED-lines light source inside a portable parallelepiped box that illuminates the surface of target. The implementation of the multispectral-box also includes a Raspberry Pi board (CPU) and camera used to collect and process the data through a user-friendly software able to produce a set of thematic maps (various spectral indices for soil and vegetation characterization). The particular design of the system coupled with a specific radiometric calibration carried-out in laboratory allows the capture of reflectance images independently of solar and atmospheric conditions.

In this paper, we describe the design of the TURF-BOX system and report results of a first experiment capturing scenes both in laboratory and field conditions.

MATERIALS AND METHODS

Hardware system description

The system was composed of a hardboard box measuring 52×58×58 cm, open at the bottom with external surfaces covered with an aluminum reflective film and the internal surfaces with white matte coating. At the interior, on the topside of the box, two inclined panels supporting LED strips, for illumination of the target, were installed (Figure 1). Panel inclination and LED strips distribution within the panel were regulated to allow a uniform illumination of the target surface in preliminary observation sessions aiming at minimizing spatial variance of images captured by the camera pointed at a blank, uniform target surface. A diffuser consisting of a white opaque polycarbonate sheet, 2 mm thick, was installed at distance from the LED strips plane, separated by 1 cm spacers.

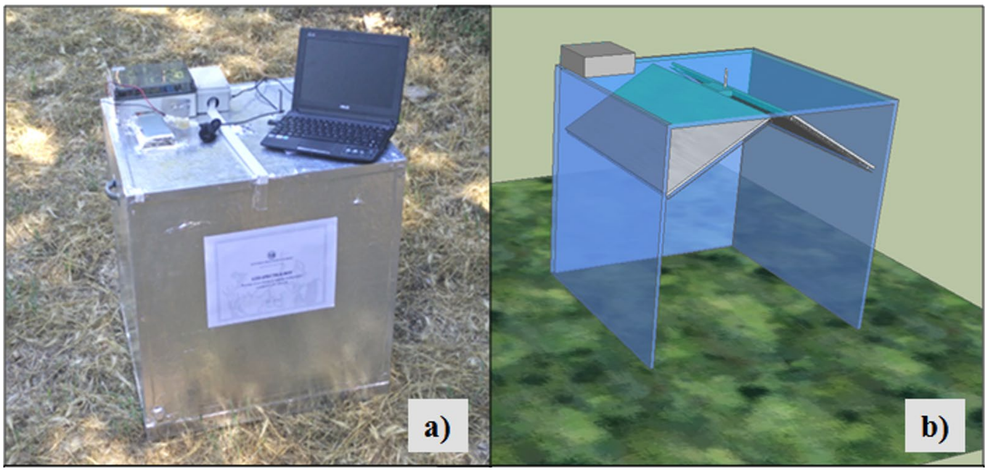

Figure 1. Overall photo (a) and details of multispectral imaging system: sketch of internal geometry (b). Light is prevented to enter from the bottom edges by a 'T-shaped' metal frame that penetrates about 1-cm into the soil.

LED lighting system consisted of three commercial monochromatic narrow-band LED strips emitting in the blue (BLED), green (GLED), red (RLED) and NIR (NIRLED) regions, at 460, 420±20, 520±20 nm with FWHM 20 nm, 630±20 nm and 830±30 nm, respectively.

A digital camera module Pi-NoIR, v1.3 (Raspberry Pi Foundation, Cambridge, UK), equipped with a OmniVision OV5647 CMOS sensor with a 2592×1944 pixels resolution sensitive in the VIS-NIR region, was installed at the center of the top side, with a supporting device consisting of a metal plate with three regulating screws for the alignment of the field of view (FOV). Camera focus was regulated for a 50 cm distance from the bottom target surface. Given the angular FOV of the camera, image captured was 50×38 cm.

Image acquisition from the digital camera and LED control, through a relay board, were both operated by a Raspberry-PI microcontroller (Raspberry Pi Foundation, Cambridge, UK) through a suitably developed control software using a web application framework written in Python language, accessible through a web-based user interface. Each acquisition consisted of four distinct RAW images captured, one for each LED type sequentially turned on.

1. Methods and algorithms for image capture and processing.

All processing is performed within the device, from image capture to RAW image data processing and calibration. In synthesis, for each of the four RAW images captured, under the four different LED light sources, the result of sub-pixel extraction from the Bayer pattern is one 1296×972 pixel image.

After extraction, each monochrome RAW image was subjected to dark frame subtraction and vignetting correction separately, using specifically developed correction matrices. In detail, a dark frame image matrix was captured at zero irradiance and taken as a baseline signal level to subtract from the RAW images. Similarly, a devignetting matrix was calculated from a flat image obtained capturing using as a target a white paper sheet uniformly illuminated by each source LED types. This allowed the calculation of an empirical camera equation, for each LED source, developed analyzing the pattern of change of signal level along four transects crossing the center of the image, were maximum signal levels are recorded.

A specific correction was developed to obtain reflectance images for each source LED type. To this aim, an empirical line approach (Wang and Myint, 2015; Chavez, 1996) was adopted by analyzing, in laboratory conditions, a collection of images acquired on calibrated targets.

Functions for the calculation of VI images from the reflectance calibrated images are implemented into the image processing tool developed within the control system. The specific VIs selected are based on VIS-NIR spectral region and at the moment the most frequently adopted (Mousaei Sanjerehei, 2014) are implemented both in the VIS-NIR domain, such as NDVI, EVI, SAVI, and in the simple VIS range (GI, GLI, VARI).

2. Setup of experimental laboratory and in-field campaigns.

Two different test were performed to assess the TURF-BOX performance: a preliminarily analysis was carried out in laboratory condition to test all the corrections and calibrations procedures implemented in the device; subsequently the TURF-BOX was tested in field conditions in the experimental farm Opera Pia Istituto Agrario Castelnuovo managed by department of Agriculture, Food and Forest Science of Palermo University.

The laboratory test was performed acquiring a set of images over 7 calibrated artificial targets characterized by different gray reflectance values, measured using an ASD FieldSpec Pro spectroradiometer (Analytical Spectral Device, Inc.), covering VIS to SWIR wavelengths (350-2500 nm).

The field campaign was carried out over 16 experimental plots measuring 1×1 m characterized by a sandy soil (75% of sand, 15% of silt and 10% of clay), medium content of organic matter, low total nitrogen and available phosphorus content. The field was divided into two parts consisting of “fertilized” and “non-fertilized” treatments. Each of these treatments was divided in eight 1-m^2 plots separated by a non-grassy strip of 0.40 m. All the plots were seeded with different doses of a perennial ryegrass (*Lolium perenne* L. ‘Ready’). Irrigation was performed through a micro-sprinkler irrigation system, suspended over the experimental plots. The sowing was carried out on 2 May 2016, and on 19 May 2016 and on 25 May on all the plots were distributed with a fertigation supply, 100 g of mineral fertilizer PK 52.34. On 10 June, nitrogen fertilization was added only for the “fertilized” treatment, incorporating 35.2 g of a 15-5-15 mineral fertilizer (Scotts Sportsmaster Municipal).

RESULTS AND DISCUSSION

Laboratory test

In Figure 2 the main results of laboratory test showed that the relationship between pixels digital number (DN) versus radiometrically-calibrated reflectance of test target panels was linear for all wavelength bands tested. Reflectance value of the test panels was chosen to enhance the linearity of the relationship within the low-reflectance range of the relationship, the condition more frequently encountered in field measurements (Figure 2, panels 1, 2, 3 and panels 4, 5, 6).

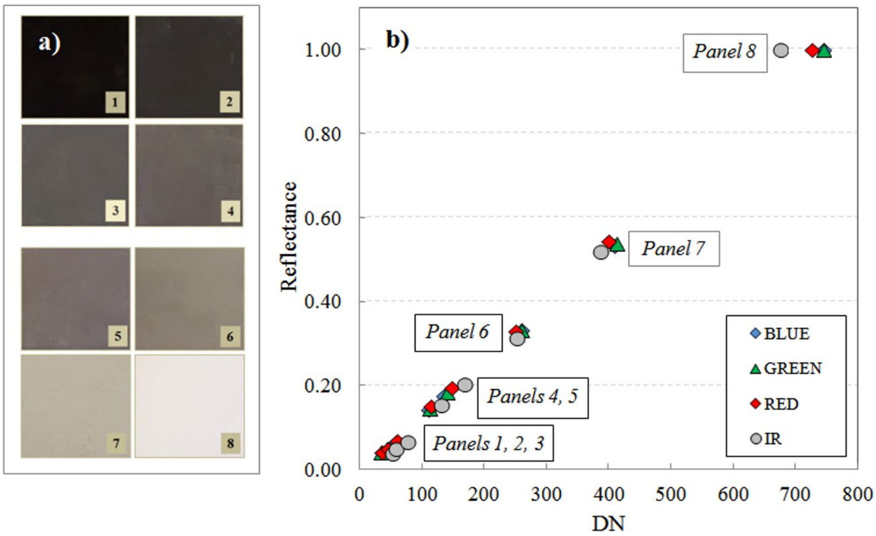

Figure 2. Relationship between pixels digital number acquired by the imaging sensor and spectrally calibrated reflectance of test targets under different monochromatic light sources.

Beside the highest reflectance values (Figure 2, panels 7 and 8), the reflectance vs. DN relationship was similar regardless the light source adopted, indicating a fairly flat spectral response of the imaging sensor adopted. Despite this, however, the calibration equations, in the subsequent calculations, were kept separated by light source.

Field test

Figure 3 shows a first result of the test carried out on June 8th 2019 when a first cut of *Lolium* seeded in the experimental boxes was achieved. In order to assess the TURF-BOX sensitivity in capturing biomass variations, the measurements were made at different levels of soil surface coverage (30 and 70%) immediately before and immediately after the cut for both "fertilized" and "non-fertilized" treatments trying to capture the same scene; in the same time the spatial distributions of the NDVI index were processed by the code implemented in the system.

The different NDVI images captured were assessed using the image-histogram technique able to determine the distributions of NDVI values for each image. The comparison between Figures 3a-3b and 3c-3d clearly shows how the NDVI image well reflected the spatial distribution variation of biomass levels between plots characterized by different fraction cover, both before and after the cut. Before cutting, in plot at 30% of fraction cover (Figure 3a), NDVI values were characterized by a mean value of 0.265 and a standard deviation of 0.24, with a typically bimodal shape distribution of image-histogram that highlights the different response in terms of NDVI between soil and the vegetation.

Differently in plot at 70% of fraction cover (Figure 3b), the mean value of NDVI resulted 0.533 with a standard deviation of 0.18; in this case the shape of image-histogram resulted unimodal as consequence of the greater uniformity in terms of spectral response.

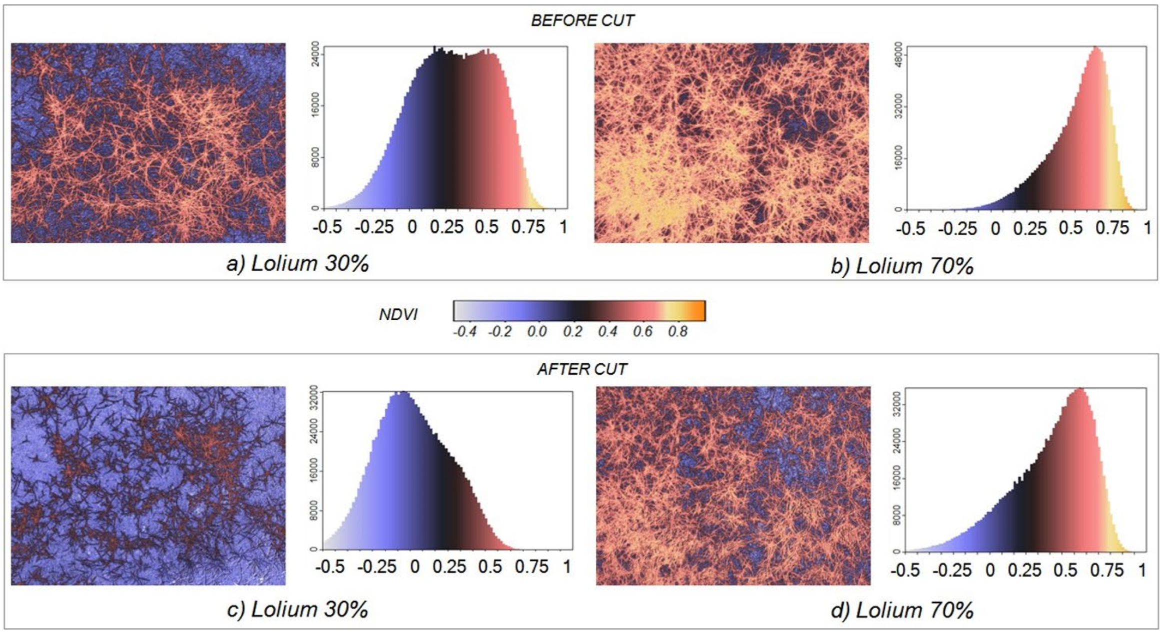

Figure 3. Spatial distributions and image-histograms of NDVI acquired from TURF-BOX at different fraction cover value and before and after the cut.

After the cut, in the plot at 30% of fraction cover (Figure 3c) the NDVI mean value decreased from 0.265 to 0.022 and the shape of image-histogram changed from bimodal to unimodal. Likewise, in the plot at 70% of fraction cover (Figure 3d), the NDVI mean value decreased from 0.533 to 0.377 while changes in the shape of image-histogram, in comparison to 30% *Lolium*, were far less important, preserving the general shape of the distribution, even if with a higher incidence of lower NDVI classes.

The aforementioned considerations find confirmation in the graphs of Figure 4 which summarizes all the results obtained from the analysis of NDVI values in all experimental plots: particularly, for different fraction cover levels, the effects of the cut in "non-fertilized" plots measured on 8th June 2019 is showed in Figure 4a where lower NDVI for all densities were detected. NDVI difference between pre and post-cut were larger in 30% *Lolium* plots, showing a higher sensitivity of NDVI in the lower range of vegetation densities, also in coherence with its intrinsic nonlinear behavior.

Figure 4b shows the effects of fertilization in terms of NDVI for a set of plots analyzed on 22th June 2019 ten days after the fertilization. The lower values of NDVI were detected for non-fertilized plots where also a reduced nonlinear behavior was observed in contrast to fertilized plot where NDVI were saturated at a density as-low-as 30% *Lolium*. As it will be better analyzed further in the text, it is also interesting to observe the high NDVI value at 0% *Lolium* in fertilized plots as a consequence of the cyanobacteria bio-crust produced after the fertilization.

Another possible application was also tested to evaluate the capability of the TURF-BOX as a tool for a fine characterization of soil and vegetation fractions as well as for an indirect estimation of soil physical properties that can be explained using radiometric indices operating in the VIS domain. Particularly, for grass or low vegetation partially covering the soil, the segmentation technique (Haralick and Shapiro, 1985) applied to NDVI values obtained with the TURF-BOX allowed to identify, with high accuracy, the bare soil from the vegetated fraction.

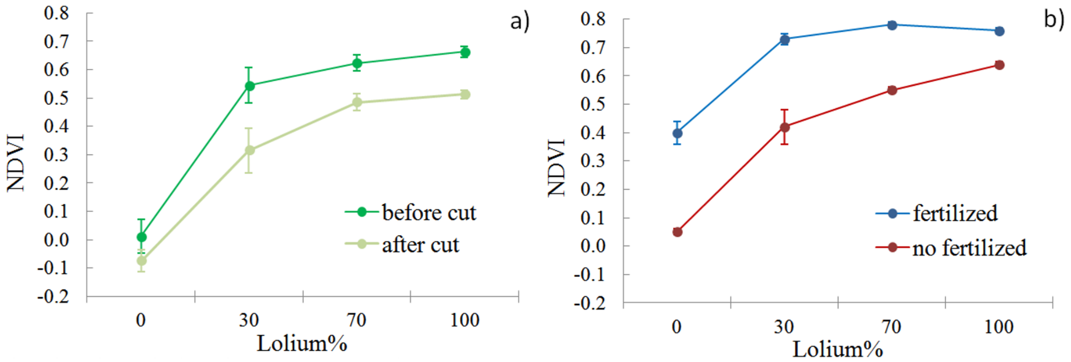

Figure 4. Effects of cut and fertilization on the NDVI measured by TURF-BOX for different *Lolium* fraction cover before and after the cut. Points in figure represent mean ± s.e.m. (n=4 in a and n=2 in b).

Figure 5 summarizes the results of the above mentioned technique applied with the TURF-BOX in the plot represented in Figure 5a and characterized by a *Lolium* fraction of 30%; starting from the image-histogram of the map of NDVI (Figure 5b) the value of 0.5 was fixed as threshold to separate bare soil (NDVI <0.5) from vegetation (NDVI >0.5). In this way two different images were retrieved representing the only bare soil (Figure 5c) and the vegetation fraction (Figure 5d).

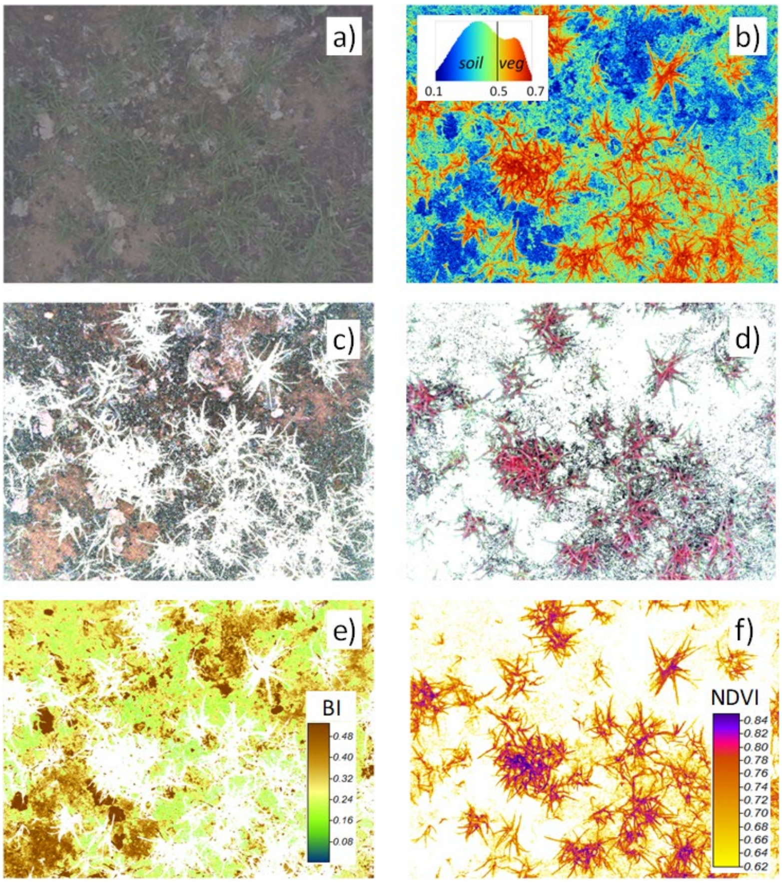

Figure 5. Results of two different techniques applied with TURF-BOX for an experimental plot (a); NDVI image (b); masked RGB image isolating the soil fraction (c); masked multispectral image visualized in RGB false color (ir = R, green = G, blu = B) (d); brightness index over bare soil (e); NDVI over vegetation (f).

Then, only for the bare soil image (Figure 5c), the so-called "Brightness Index", BI, was computed (Figure 5e) combining the calibrated VIS-NIR bands of TURF-BOX and according the algorithm proposed by Huete and Escadafal (1991) with the aim to evaluate the presence of salts and/or organic contaminants in soils. Differently, for the image of the only vegetation (Figure 5d) the NDVI image was obtained (Figure 5f).

These results and particularly the outputs plotted in Figure 5e and 5f clearly show the potentiality of TURF-BOX as a low-cost tool for applications in support of precision agriculture in grass and/or small vegetation conditions. In fact, in addition to the estimate of the vegetative vigor provided by the NDVI and other vegetation indices, it is interesting to note that the areas characterized by higher brightness index (BI >0.4) allowed to detect parts of soil probably characterized by the presence of a cyano-bacteria bio-crust that usually produce a higher brightness in the soil.

CONCLUSIONS

The instrument presented in the paper, called TURF-BOX, can be considered a new low cost (<€150) multispectral camera prototype operating in the VIS-NIR domain aimed at monitoring different types of natural surfaces. The use of LED technology sources operating on specific wavelengths (3 bands in the visible and one in the near infrared). The output measurements of TURF-BOX consist of radiometrically corrected reflectance images in the VIS-NIR spectral domain, both in the form of images (thematic maps of vegetation indexes) and in numeric format (values associated with the pixels of the image and statistical graphs of the distributions of the values measured in the recovery area).

A user-friendly software implemented in TURF-BOX allows the user to control the instrument producing a set of thematic maps (various spectral indices for soil and vegetation characterization). A preliminary test of TURF-BOX functioning, carried out in both laboratory and field conditions, produced good results in monitoring different characteristics of a short grass such as, vigor, fraction cover, fertilization and also to detected anomalies is the top surface of a bare soil. The aforementioned innovative features make TURF-BOX an alternative or integrative system of current technical precision monitoring and proximal-sensing.

Literature cited

Aparicio, N., Villegas, D., Casadesus, J., Araus, J.L., and Royo, C. (2000). Spectral vegetation indices as non-destructive tools for determining durum wheat yield. Agron. J. *92* (*1*), 83–91 https://doi.org/10.2134/agronj2000.92183x.

Berra, E.F., Gaulton, R., and Barr, S. (2016). Use of a digital camera onboard a UAV to monitor spring phenology at individual tree level. Paper presented at: IEEE International Geoscience and Remote Sensing Symposium (Bejing, China: IEEE).

Chavez, P.S. (1996). Image-based atmospheric corrections revisited and improved. Photogramm. Eng. Remote Sensing *62*, 1025–1036.

Haralick, R.M., and Shapiro, L.G. (1985). Image segmentation techniques. Comput. Vision Graph. *29* (*1*), 100–132 https://doi.org/10.1016/S0734-189X(85)90153-7.

Huete, A.R., and Escadafal, R. (1991). Assessment of biophysical soil properties through spectral decomposition techniques. Remote Sens. Environ. *35* (*2–3*), 149–159 https://doi.org/10.1016/0034-4257(91)90008-T.

Maltese, A., Minacapilli, M., Cammalleri, C., Ciraolo, G., and D'Asaro, F. (2010). A thermal inertia model for soil water content retrieval using thermal and multispectral images. Paper presented at: The International Society for Optical Engineering (Bellingham, Washington, USA: SPIE).

Mousaei Sanjerehei, M. (2014). Assessment of spectral vegetation indices for estimating vegetation cover in arid and semiarid shrublands. Range Manag. Agrofor. *35* (*1*), 91–100.

Viscarra Rossel, R.A., McGlynn, R.N., and McBratney, A.B. (2006). Determing the composition of mineral-organic mixes using UV-vis-NIR diffuse reflectance spectroscopy. Geoderma *137* (*1-2*), 70–82 https://doi.org/10.1016/j.geoderma.2006.07.004.

Wang, C., and Myint, S.W. (2015). A simplified empirical line method of radiometric calibration for small unmanned aircraft systems-based remote sensing. IEEE J. Sel. Top. Appl. Earth Obs. Remote Sens. *8* (*5*), 1876–

https://doi.org/10.1109/JSTARS.2015.2422716.